Electronic Supplementary Material (ESI) for RSC Advances.

Supporting Information

for the manuscript entitled

Transition metal induced switch of fluorescence and absorption responses of Zn(II)porphyrin-DNA conjugate to cysteine derivatives

Jung Kyu Choi, Gevorg Sargsyan, Breiana D. Johnson, Milan Balaz*

University of Wyoming, Department of Chemistry, Laramie, WY 82071, USA

E-mail: mbalaz@uwyo.edu

ESI: Table of Contents

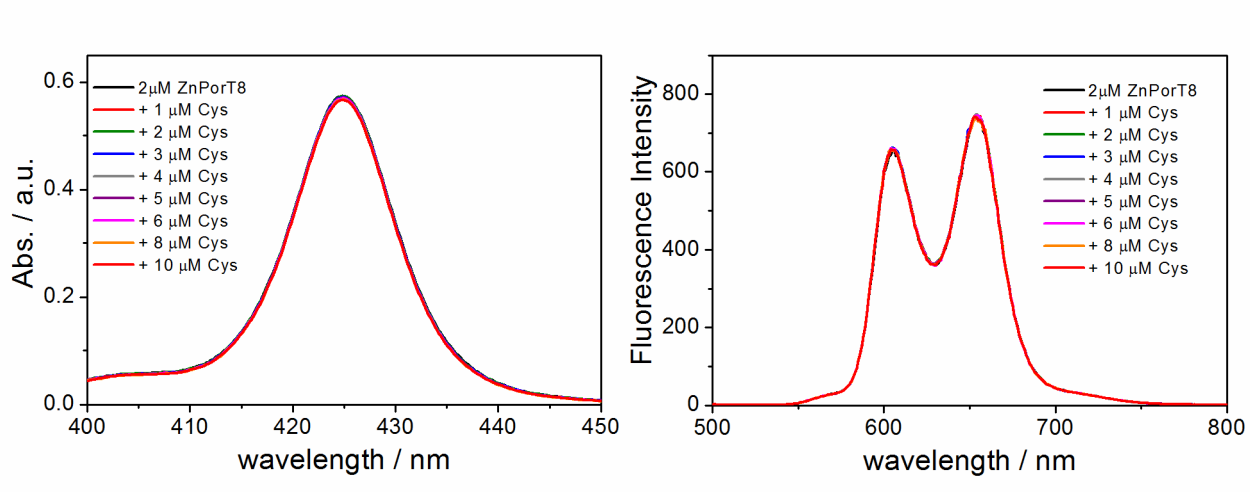

Figure S1. UV-vis absorption (left) and emission (right) spectra of the **ZnPorT8** (2μM) upon stepwise addition of the cysteine (Cys) from 1 to 10 μM in Na-cacodylate buffer (1 mM, pH = 7.0, 20 °C).

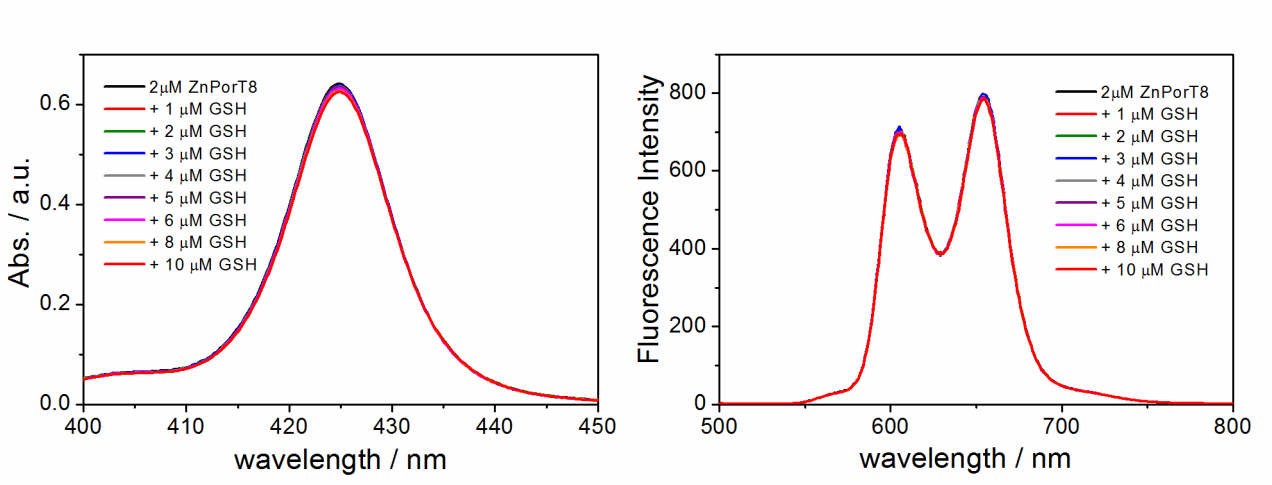

Figure S2. UV-vis absorption (left) and emission (right) spectra of the **ZnPorT8** (2μM) upon stepwise addition of the glutathione (GSH) from 1 to 10 μM in Na-cacodylate buffer (1 mM, pH = 7.0, 20 °C).

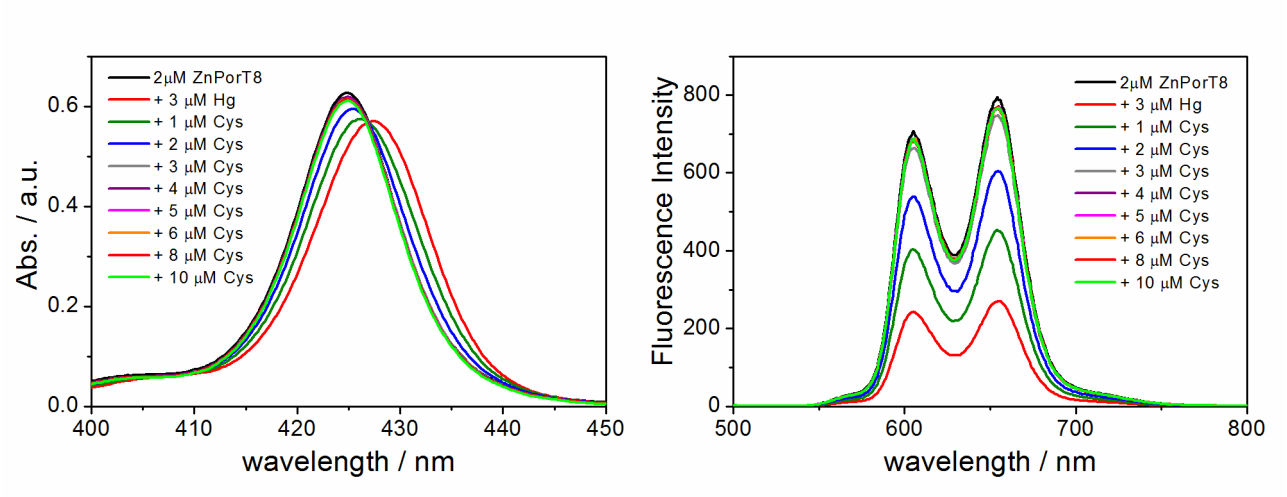

Figure S3. UV-vis absorption (left) and emission (right) spectra of the **ZnPorT8**/Hg^{2+} complex (2.0 μM of **ZnPorT8** and 3.0 μM of Hg^{2+} ion) upon stepwise addition of the cysteine (Cys) from 1 to 10 μM in Na-cacodylate buffer (1 mM, pH = 7.0, 20 °C).

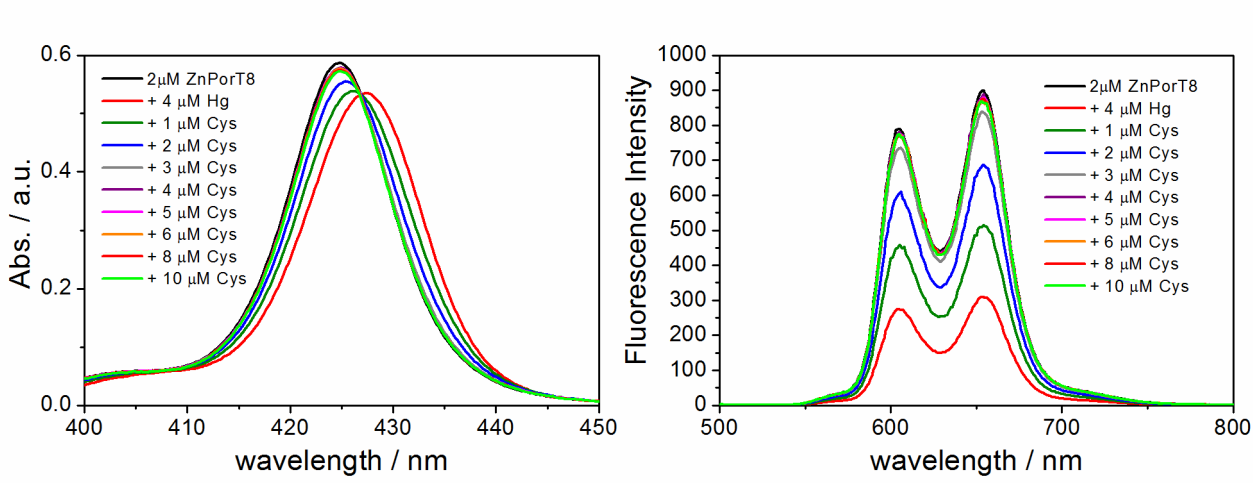

Figure S4. UV-vis absorption (left) and emission (right) spectra of the **ZnPorT8**/Hg^{2+} complex (2.0 μM of **ZnPorT8** and 4.0 μM of Hg^{2+} ion) upon stepwise addition of the cysteine (Cys) from 1 to 10 μM in Na-cacodylate buffer (1 mM, pH = 7.0, 20 °C).

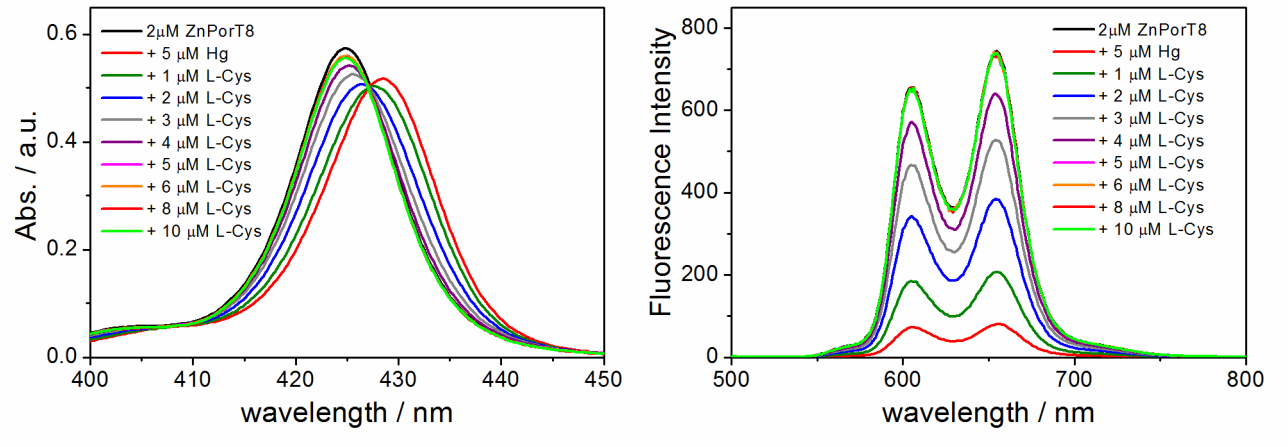

Figure S5. UV-vis absorption (left) and emission (right) spectra of the **ZnPorT8**/Hg^{2+} complex (2.0 μM of **ZnPorT8** and 5.0 μM of Hg^{2+} ion) upon stepwise addition of the L-cysteine (L-Cys) from 1 to 10 μM in Na-cacodylate buffer (1 mM, pH = 7.0, 20 °C).

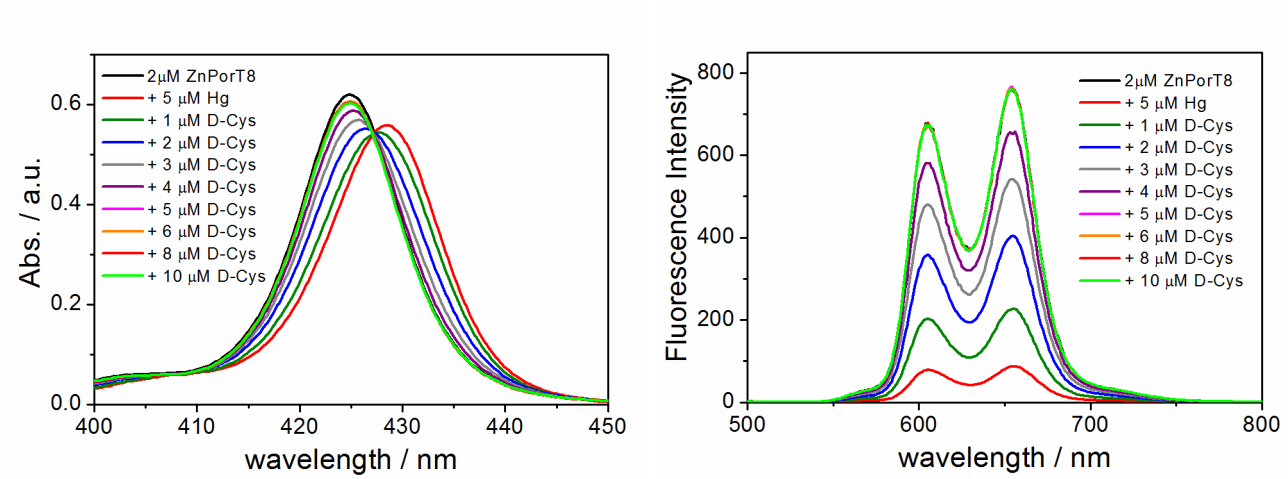

Figure S6. UV-vis absorption (left) and emission (right) spectra of the **ZnPorT8**/Hg^{2+} complex (2.0 μM of **ZnPorT8** and 5.0 μM of Hg^{2+} ion) upon stepwise addition of the D-cysteine (D-Cys) from 1 to 10 μM in Na-cacodylate buffer (1 mM, pH = 7.0, 20 °C).

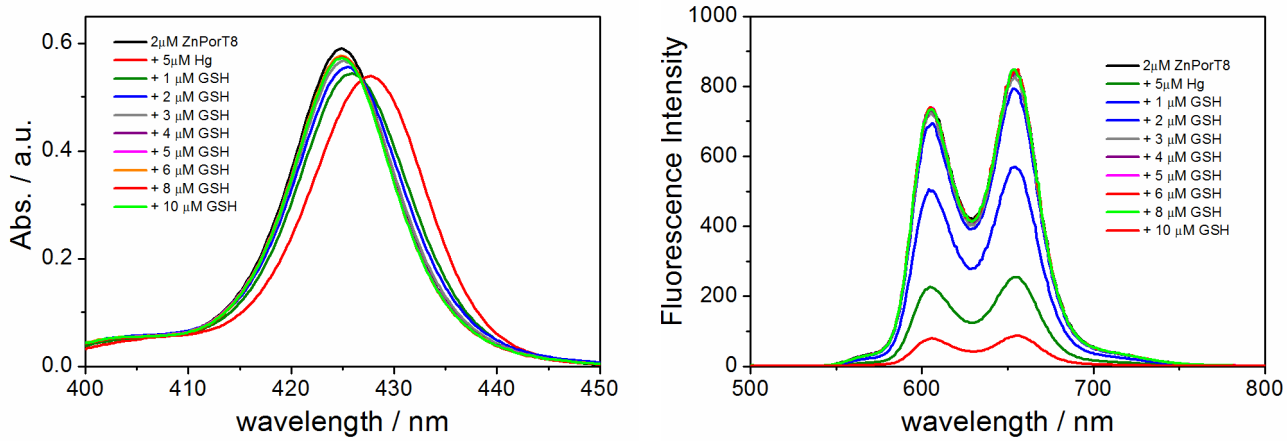

Figure S7. UV-vis absorption (left) and emission (right) spectra of the **ZnPorT8**/Hg^{2+} complex (2.0 μM of **ZnPorT8** and 5.0 μM of Hg^{2+} ion) upon stepwise addition of the Glutathione (GSH) from 1 to 10 μM in Na-cacodylate buffer (1 mM, pH = 7.0, 20 °C).

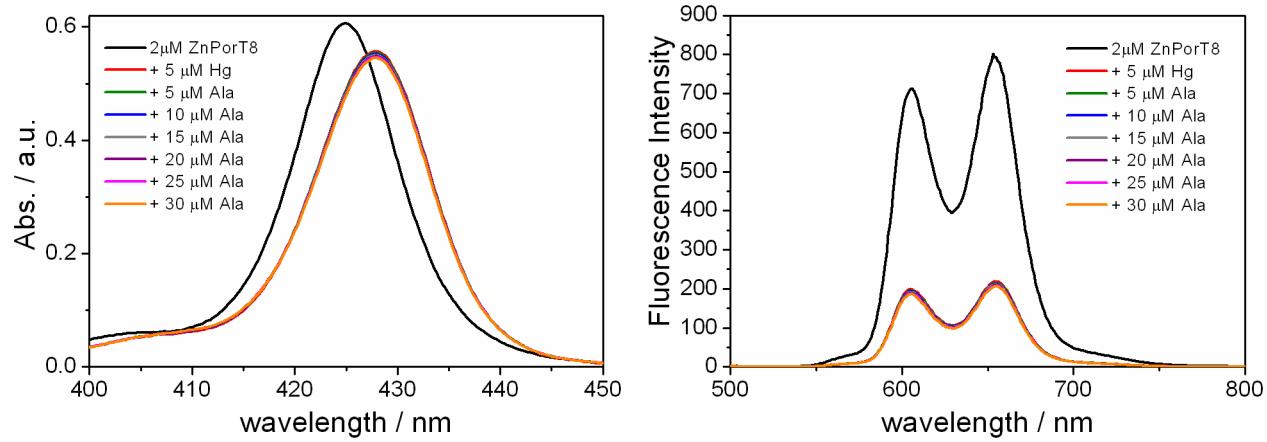

Figure S8. UV-vis absorption (left) and emission (right) spectra of the **ZnPorT8**/Hg^{2+} complex (2.0 μM of **ZnPorT8** and 5.0 μM of Hg^{2+} ion) upon stepwise addition of the alanine (Ala) from 5 to 30 μM in Na-cacodylate buffer (1 mM, pH = 7.0, 20 °C).

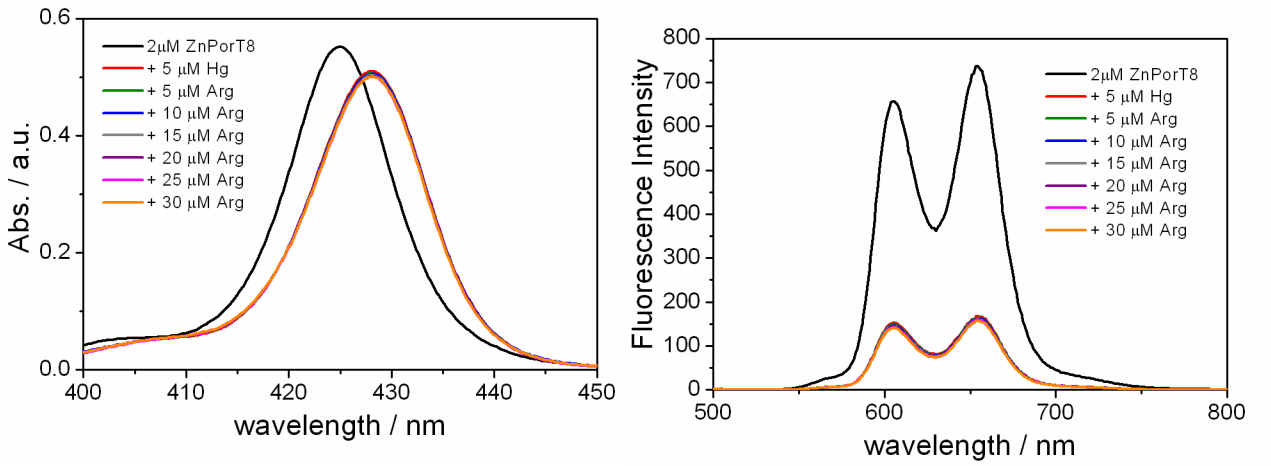

Figure S9. UV-vis absorption (left) and emission (right) spectra of the **ZnPorT8**/Hg^{2+} complex (2.0 μM of **ZnPorT8** and 5.0 μM of Hg^{2+} ion) upon stepwise addition of the arginine (Arg) from 5 to 30 μM in Na-cacodylate buffer (1 mM, pH = 7.0, 20 °C).

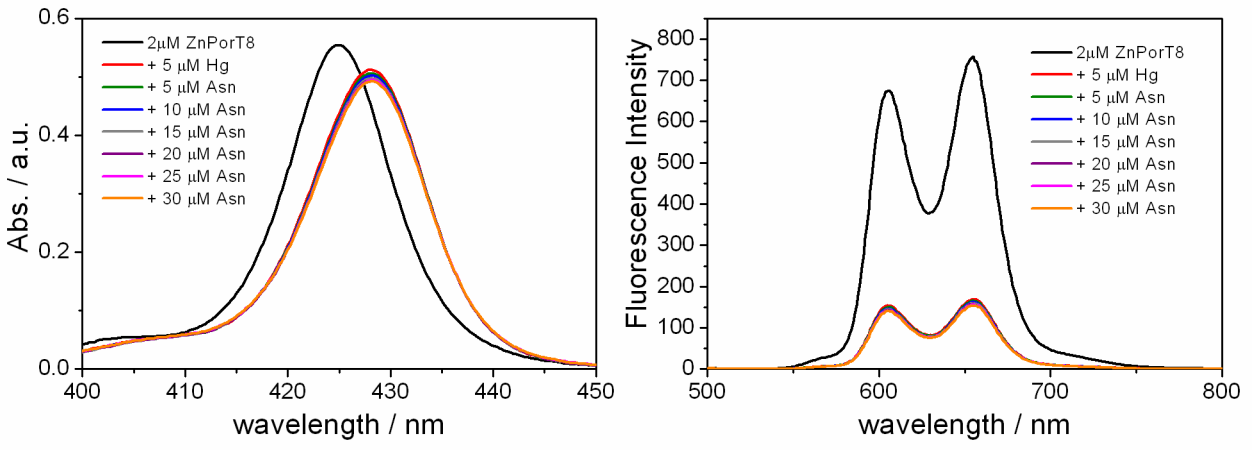

Figure S10. UV-vis absorption (left) and emission (right) spectra of the **ZnPorT8**/Hg^{2+} complex (2.0 μM of **ZnPorT8** and 5.0 μM of Hg^{2+} ion) upon stepwise addition of the aspartic acid (Asn) from 5 to 30 μM in Na-cacodylate buffer (1 mM, pH = 7.0, 20 °C).

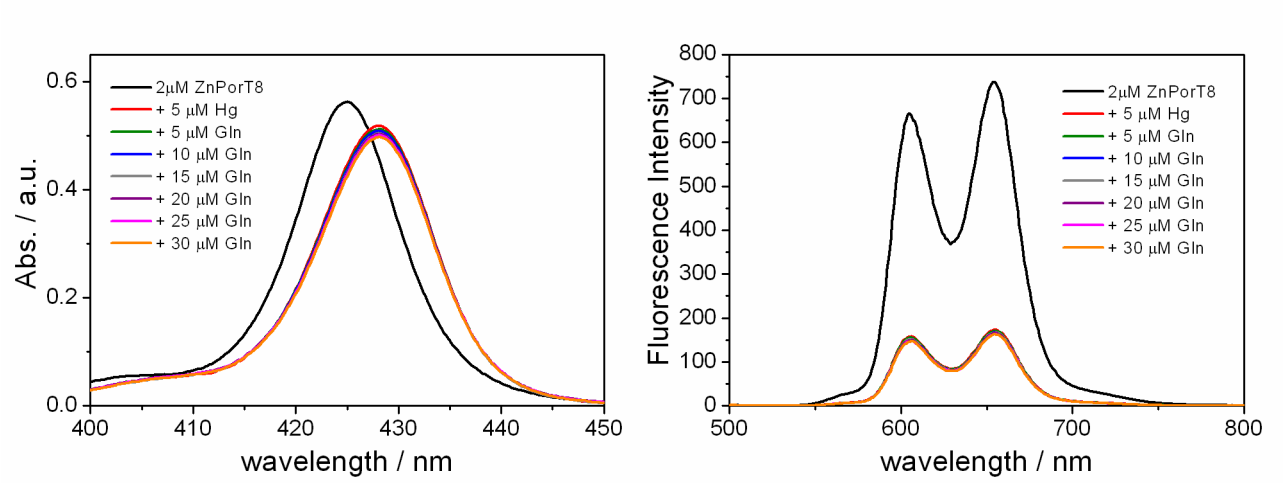

Figure S11. UV-vis absorption (left) and emission (right) spectra of the **ZnPorT8**/Hg^{2+} complex (2.0 μM of **ZnPorT8** and 5.0 μM of Hg^{2+} ion) upon stepwise addition of the glutamic acid (Gln) from 5 to 30 μM in Na-cacodylate buffer (1 mM, pH = 7.0, 20 °C).

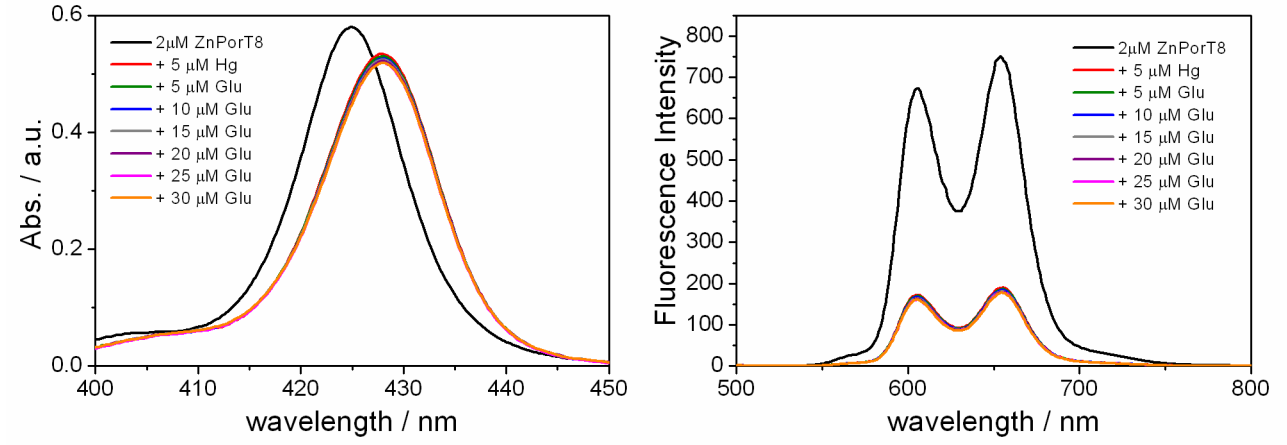

Figure S12. UV-vis absorption (left) and emission (right) spectra of the **ZnPorT8**/Hg^{2+} complex (2.0 μM of **ZnPorT8** and 5.0 μM of Hg^{2+} ion) upon stepwise addition of the glutamine (Glu) from 5 to 30 μM in Na-cacodylate buffer (1 mM, pH = 7.0, 20 °C).

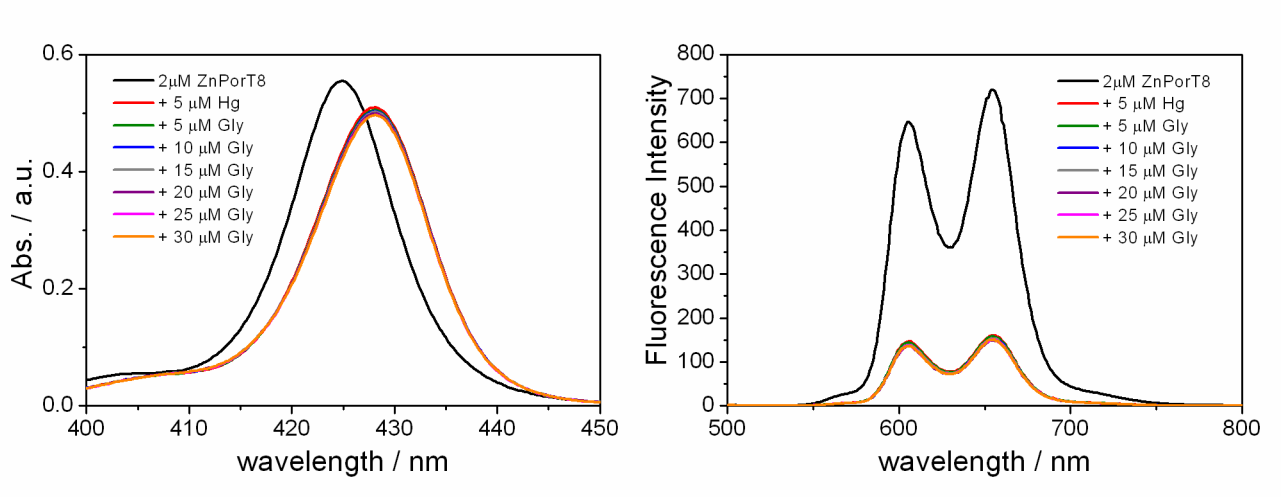

Figure S13. UV-vis absorption (left) and emission (right) spectra of the **ZnPorT8**/Hg^{2+} complex (2.0 μM of **ZnPorT8** and 5.0 μM of Hg^{2+} ion) upon stepwise addition of the glycine (Gly) from 5 to 30 μM in Na-cacodylate buffer (1 mM, pH = 7.0, 20 °C).

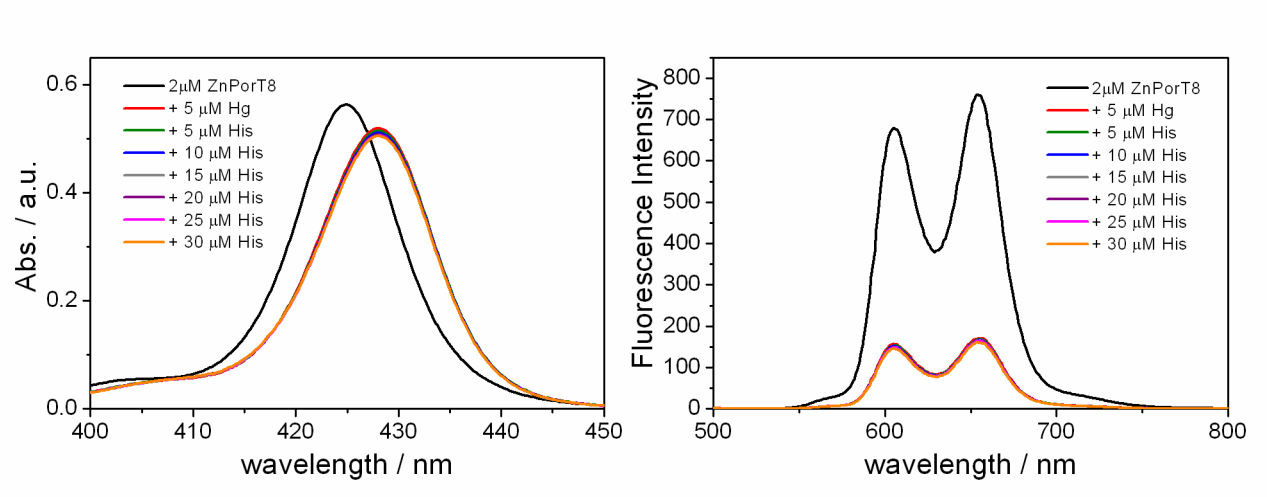

Figure S14. UV-vis absorption (left) and emission (right) spectra of the **ZnPorT8**/Hg^{2+} complex (2.0 μM of **ZnPorT8** and 5.0 μM of Hg^{2+} ion) upon stepwise addition of the Histidine (His) from 5 to 30 μM in Na-cacodylate buffer (1 mM, pH = 7.0, 20 °C).

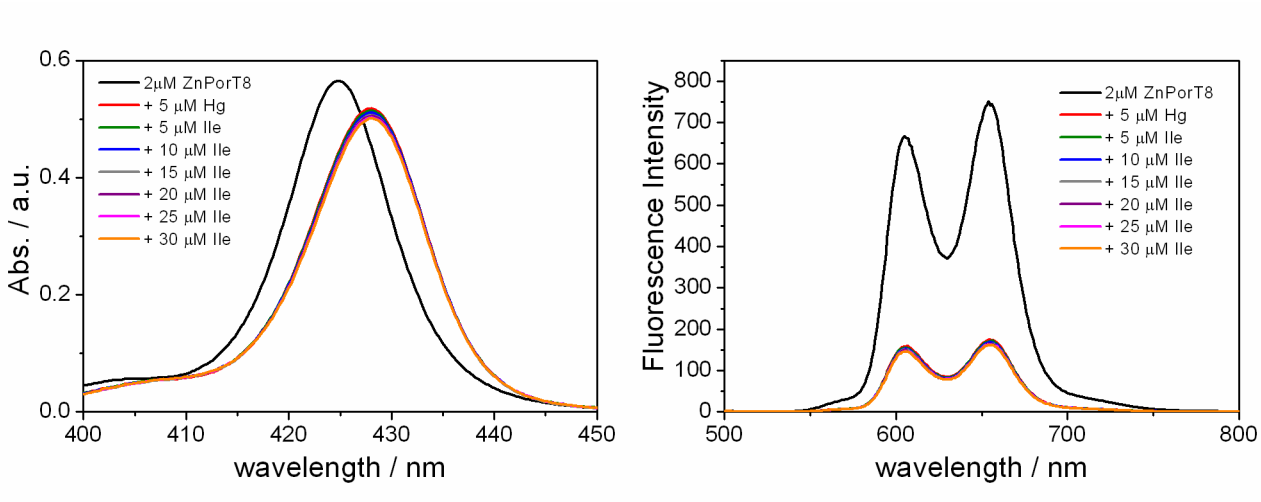

Figure S15. UV-vis absorption (left) and emission (right) spectra of the **ZnPorT8**/Hg^{2+} complex (2.0 μM of **ZnPorT8** and 5.0 μM of Hg^{2+} ion) upon stepwise addition of the iso-leucine (Ile) from 5 to 30 μM in Na-cacodylate buffer (1 mM, pH = 7.0, 20 °C).

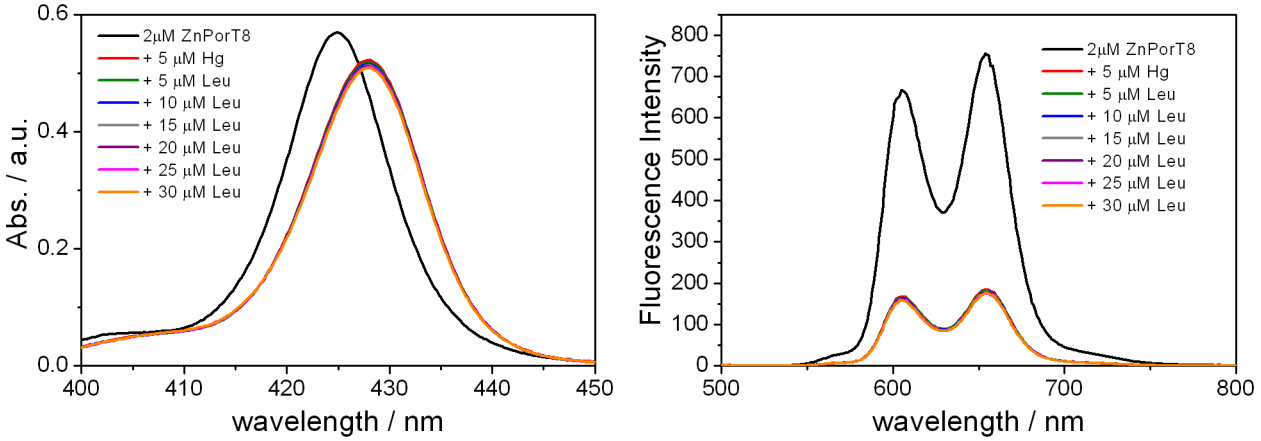

Figure S16. UV-vis absorption (left) and emission (right) spectra of the **ZnPorT8**/Hg^{2+} complex (2.0 μM of **ZnPorT8** and 5.0 μM of Hg^{2+} ion) upon stepwise addition of the leucine (Leu) from 5 to 30 μM in Na-cacodylate buffer (1 mM, pH = 7.0, 20 °C).

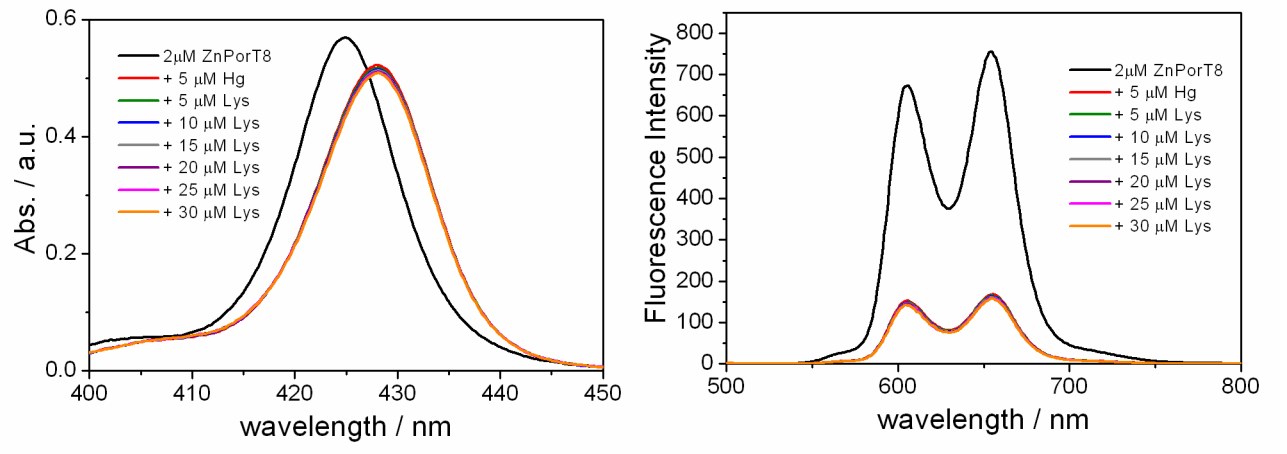

Figure S17. UV-vis absorption (left) and emission (right) spectra of the **ZnPorT8**/Hg^{2+} complex (2.0 μM of **ZnPorT8** and 5.0 μM of Hg^{2+} ion) upon stepwise addition of the lysine (Lys) from 5 to 30 μM in Na-cacodylate buffer (1 mM, pH = 7.0, 20 °C).

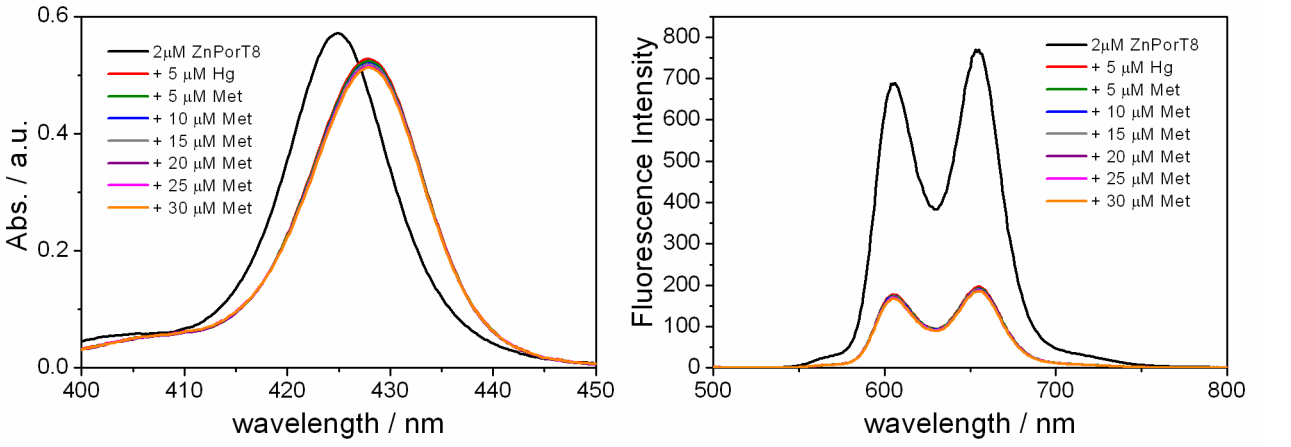

Figure S18. UV-vis absorption (left) and emission (right) spectra of the **ZnPorT8**/Hg^{2+} complex (2.0 μM of **ZnPorT8** and 5.0 μM of Hg^{2+} ion) upon stepwise addition of the methionine (Met) from 5 to 30 μM in Na-cacodylate buffer (1 mM, pH = 7.0, 20 °C).

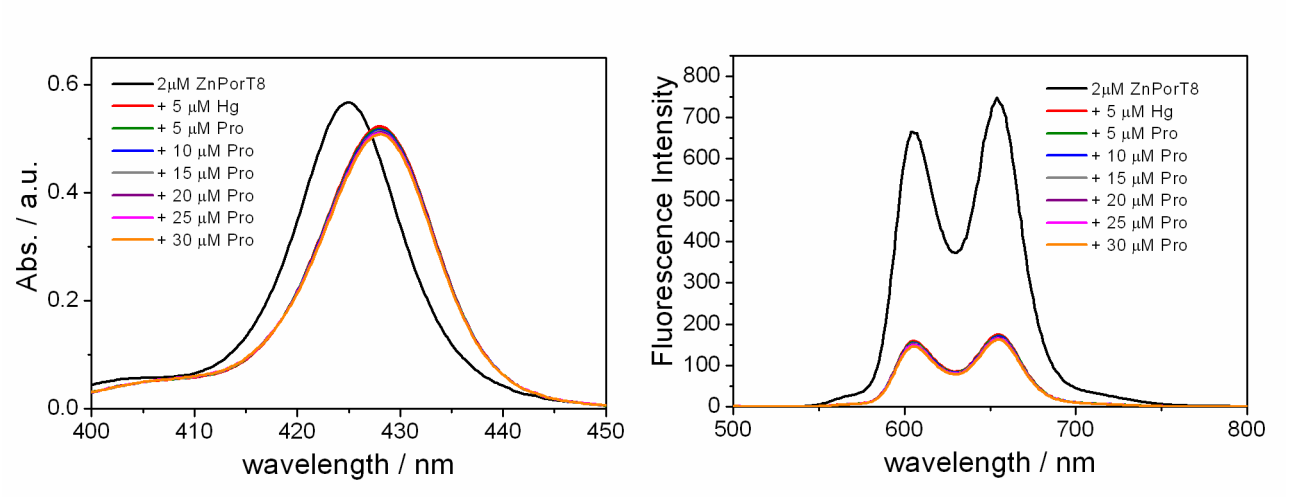

Figure S19. UV-vis absorption (left) and emission (right) spectra of the **ZnPorT8**/Hg^{2+} complex (2.0 μM of **ZnPorT8** and 5.0 μM of Hg^{2+} ion) upon stepwise addition of the proline (Pro) from 5 to 30 μM in Na-cacodylate buffer (1 mM, pH = 7.0, 20 °C).

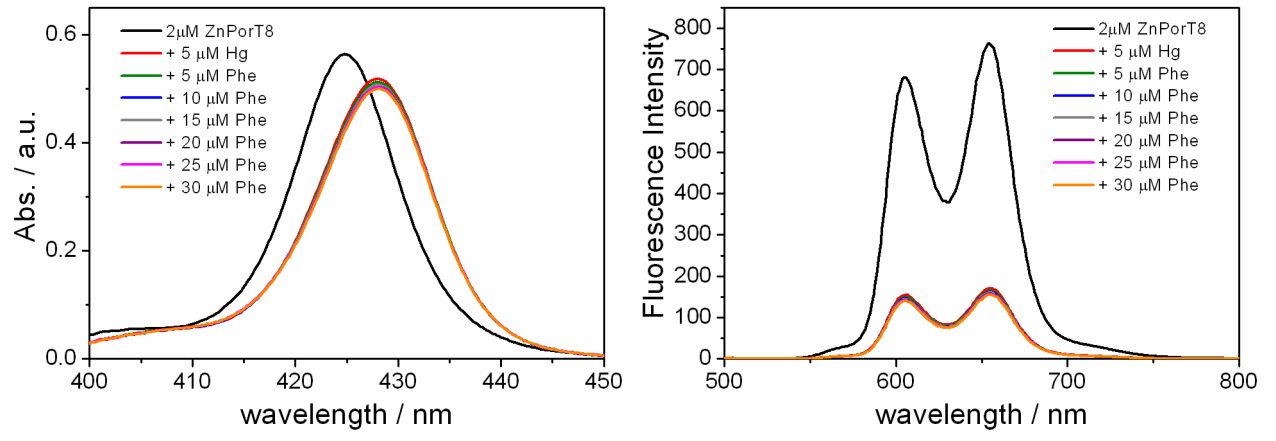

Figure S20. UV-vis absorption (left) and emission (right) spectra of the **ZnPorT8**/Hg^{2+} complex (2.0 μM of **ZnPorT8** and 5.0 μM of Hg^{2+} ion) upon stepwise addition of the phenylalanine (Phe) from 5 to 30 μM in Na-cacodylate buffer (1 mM, pH = 7.0, 20 °C).

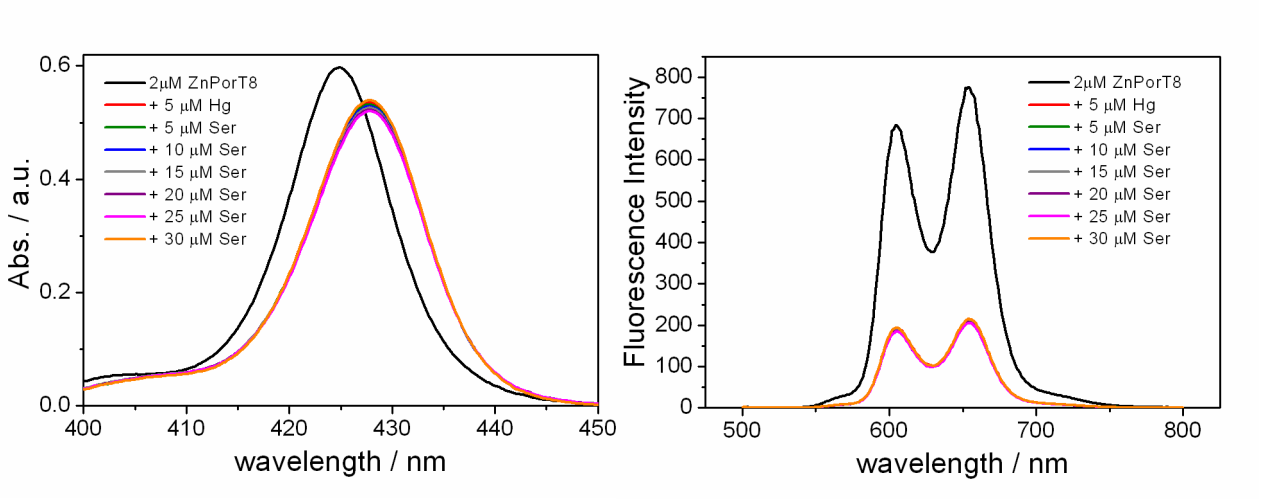

Figure S21. UV-vis absorption (left) and emission (right) spectra of the **ZnPorT8**/Hg^{2+} complex (2.0 μM of **ZnPorT8** and 5.0 μM of Hg^{2+} ion) upon stepwise addition of the serine (Ser) from 5 to 30 μM in Na-cacodylate buffer (1 mM, pH = 7.0, 20 °C).

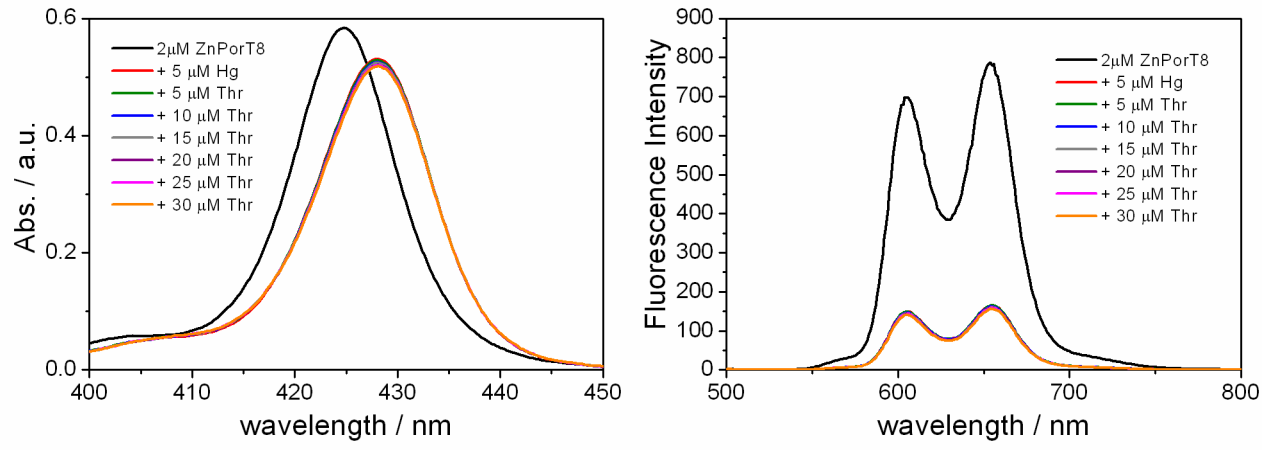

Figure S22. UV-vis absorption (left) and emission (right) spectra of the **ZnPorT8**/Hg^{2+} complex (2.0 μM of **ZnPorT8** and 5.0 μM of Hg^{2+} ion) upon stepwise addition of the threonine (Thr) from 5 to 30 μM in Na-cacodylate buffer (1 mM, pH = 7.0, 20 °C).

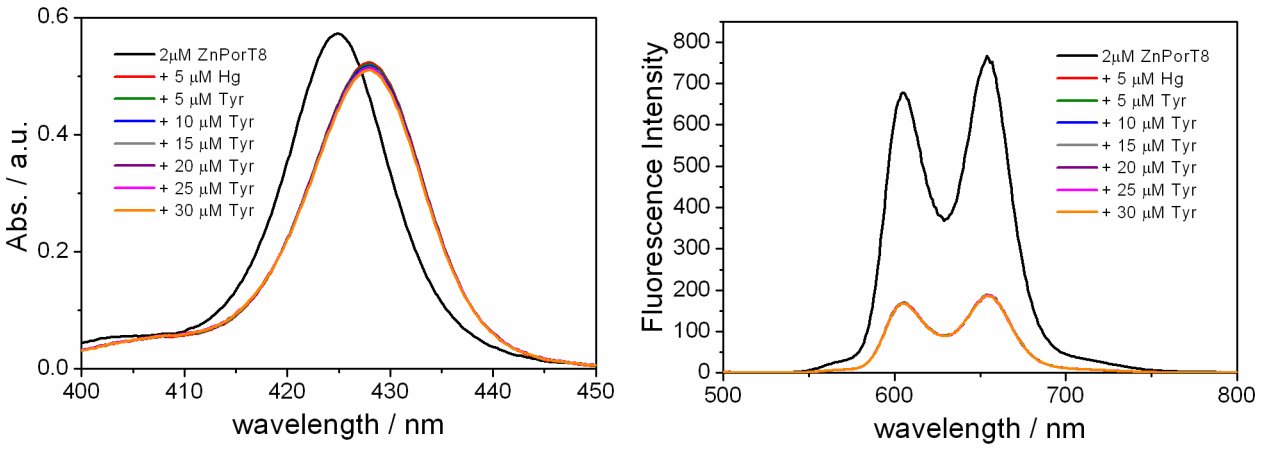

Figure S23. UV-vis absorption (left) and emission (right) spectra of the **ZnPorT8**/Hg^{2+} complex (2.0 μM of **ZnPorT8** and 5.0 μM of Hg^{2+} ion) upon stepwise addition of the tyrosine (Tyr) from 5 to 30 μM in Na-cacodylate buffer (1 mM, pH = 7.0, 20 °C).

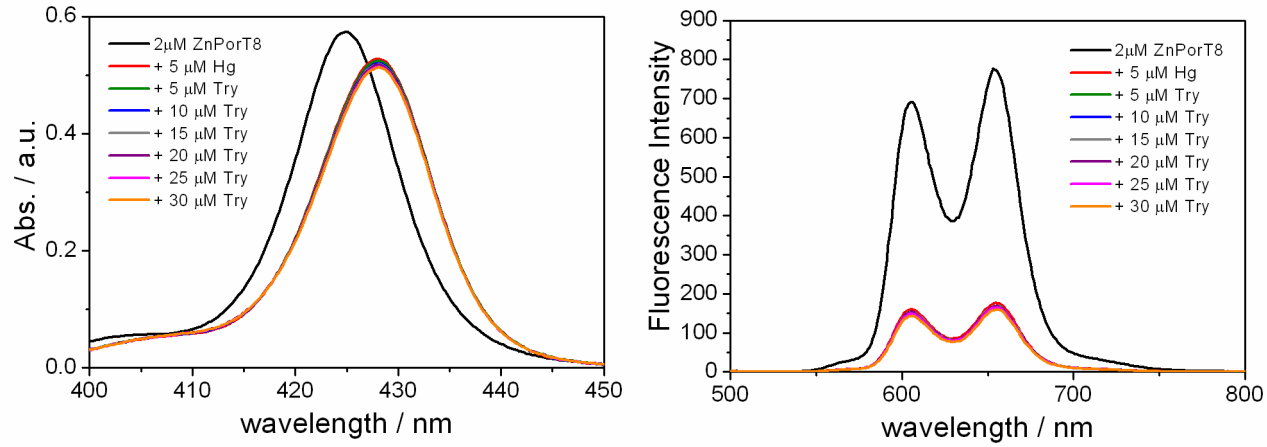

Figure S24. UV-vis absorption (left) and emission (right) spectra of the **ZnPorT8**/Hg^{2+} complex (2.0 μM of **ZnPorT8** and 5.0 μM of Hg^{2+} ion) upon stepwise addition of the tryptophan (Trp) from 5 to 30 μM in Na-cacodylate buffer (1 mM, pH = 7.0, 20 °C).

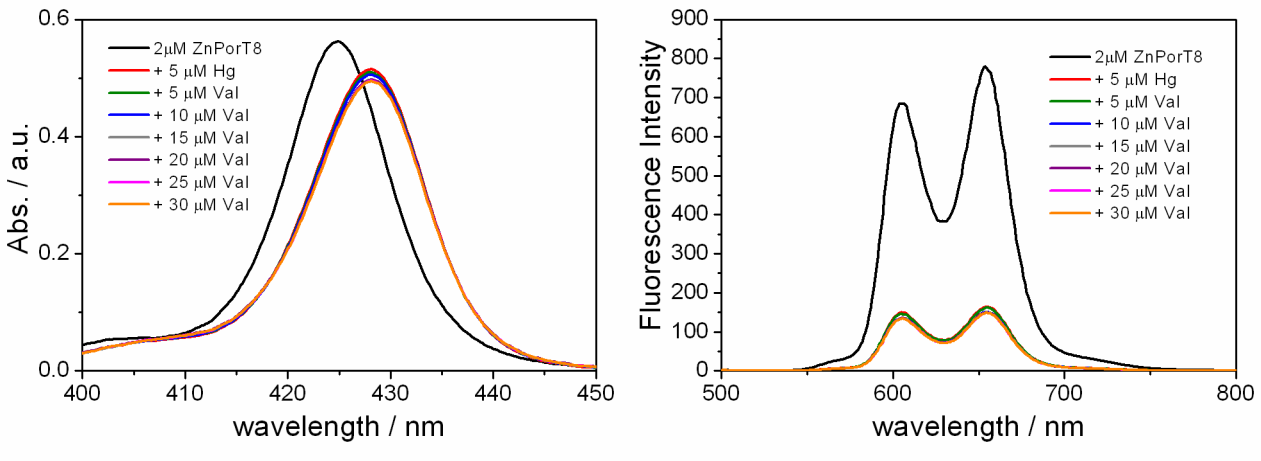

Figure S25. UV-vis absorption (left) and emission (right) spectra of the **ZnPorT8**/Hg^{2+} complex (2.0 μM of **ZnPorT8** and 5.0 μM of Hg^{2+} ion) upon stepwise addition of the valine (Val) from 5 to 30 μM in Na-cacodylate buffer (1 mM, pH = 7.0, 20 °C).

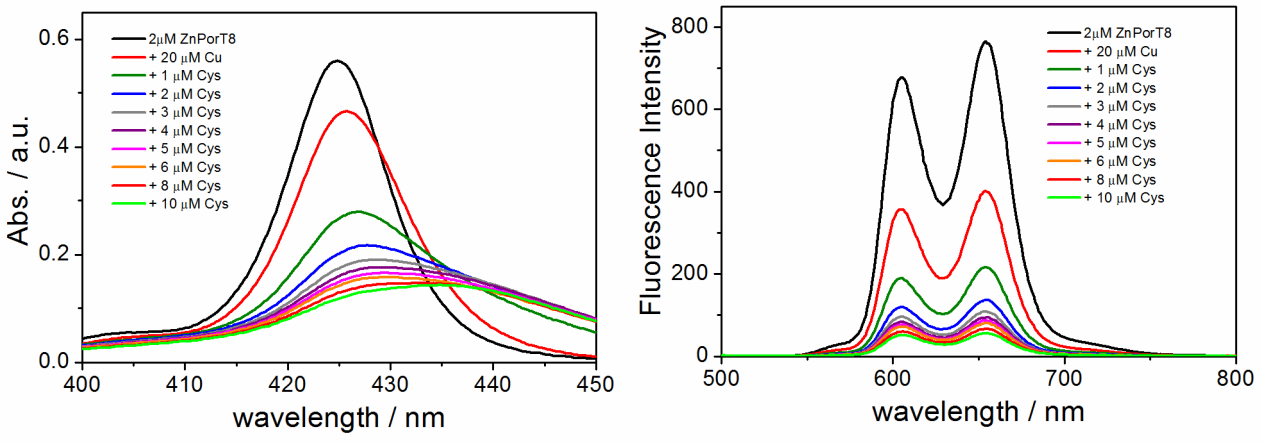

Figure S26. UV-vis absorption (left) and emission (right) spectra of the **ZnPorT8**/Cu^{2+} complex (2.0 μM of **ZnPorT8** and 20.0 μM of Cu^{2+} ion) upon stepwise addition of the cysteine (Cys) from 1 to 10 μM in Na-cacodylate buffer (1 mM, pH = 7.0, 20 °C).

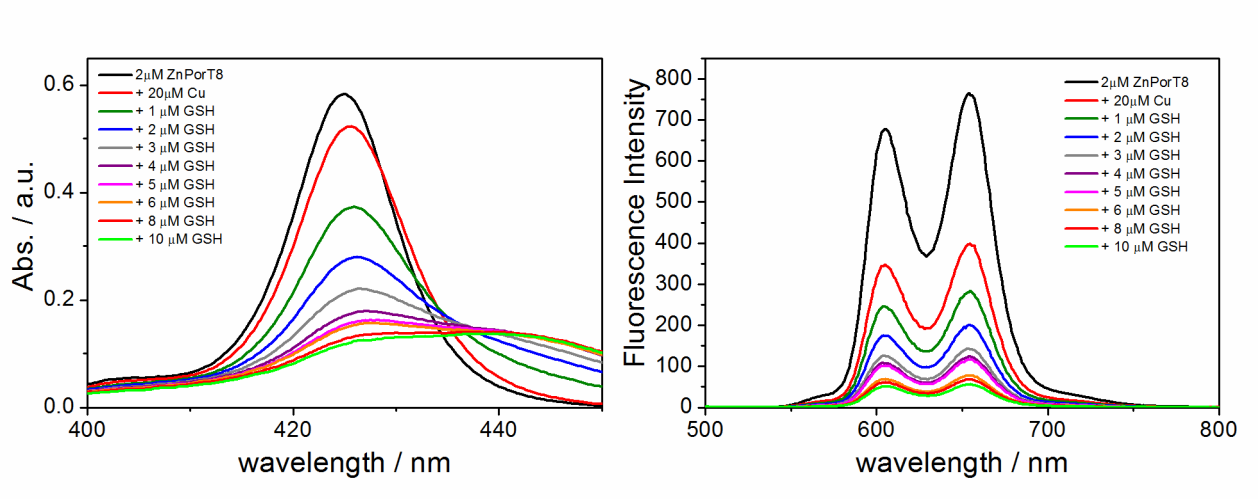

Figure S27. UV-vis absorption (left) and emission (right) spectra of the **ZnPorT8**/Cu^{2+} complex (2.0 μM of **ZnPorT8** and 20.0 μM of Cu^{2+} ion) upon stepwise addition of the Glutathione (GSH) from 1 to 10 μM in Na-cacodylate buffer (1 mM, pH = 7.0, 20 °C).

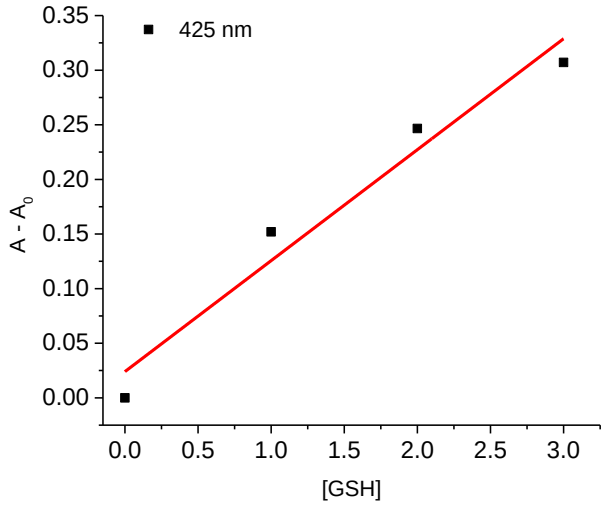

Figure S28. UV-vis absorption changes of the **ZnPorT8**/Cu^{2+} complex at 425.0 nm as a function of the GSH concentration ($A-A_0$, A_0: absorbance of **ZnPorT8**/Cu^{2+}, A: absorbance of **ZnPorT8**/Cu^{2+} after addition of GSH).

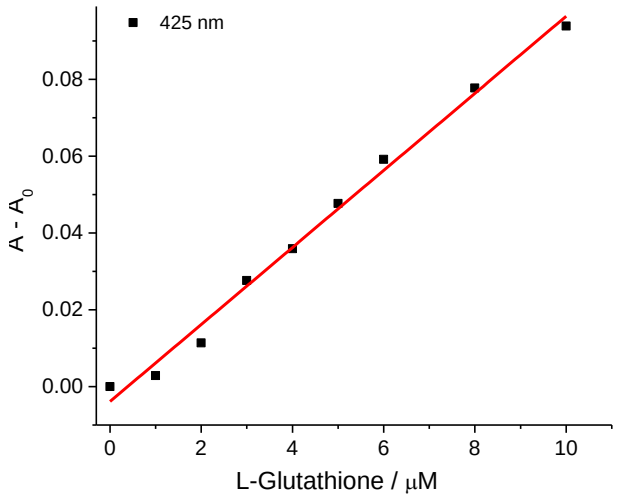

Figure S29. UV-vis absorption changes of the **ZnPorT8**/Hg^{2+} complex at 425.0 nm as a function of the GSH concentration ($A-A_0$, A_0: absorbance of **ZnPorT8**/Hg^{2+}, A: absorbance of **ZnPorT8**/Hg^{2+} after addition of GSH).

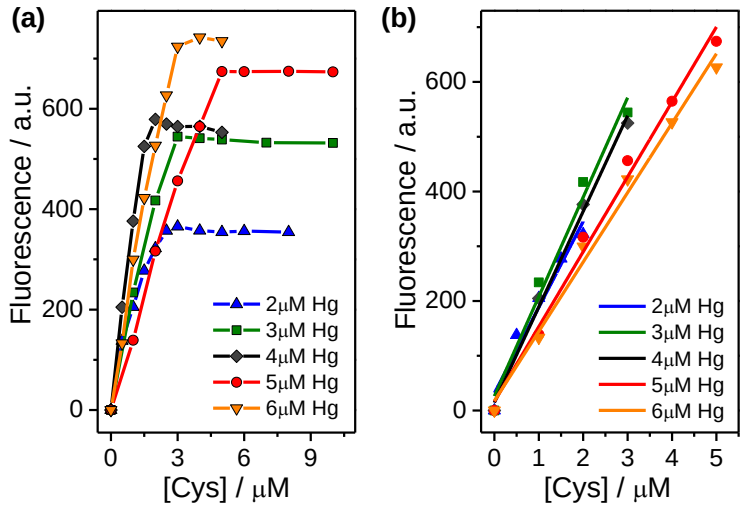

Figure S30. (a) Changes of fluorescence intensity of the **ZnPorT8**/Hg^{2+} systems ([**ZnPorT8**] = 2.0 μM, [Hg^{2+}] = 2.0 μM: blue line, 3.0 μM: green line, 4.0 μM: black line, 5.0 μM: red line, and 6.0 μM: orange line) at 654.0 nm as a function of the L-Cys concentration (0 to 10.0 μM in 1.0 μM addition steps). (b) Fluorescence intensity changes of the **ZnPorT8**/Hg^{2+} systems as a function of the L-Cys concentration (0 to 5.0 μM) detected at 654.0 nm and their linear fits (colored lines, $F-F_0$, F_0: fluorescence intensity of **ZnPorT8**/Hg^{2+}, F: fluorescence intensity **ZnPorT8**/Hg^{2+} after addition of L-Cys).

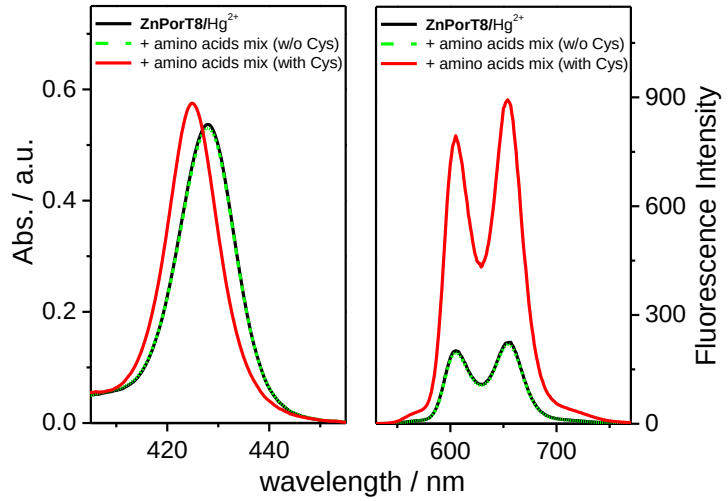

Figure S31. a) UV/Vis absorption and b) emission (λ_{exc} = 425 nm) spectra of the **ZnPorT8**/Hg^{2+} complex (black curve, [**ZnPorT8**] = 2.0 μM, [Hg^{2+}] = 5.0 μM) in the presence of an amino acid mixture (Ala, Lys, Met, Pro and Trp; each 5.0 μM) with 5.0 μM L-Cys (red curve) and without L-Cys (green dashed curve).

Table S1. Relative fluorescence quantum yields of **ZnPorT8**, **ZnPorT8**/Hg(II), and **ZnPorT8**/Cu(II).

system	[ZnPorT8]	[M(II)]	ΦF_{rel}
ZnPorT8	2 μM	--	1.0
ZnPorT8/Hg(II)	2 μM	5 μM	0.06
ZnPorT8/Cu(II)	2 μM	5 μM	0.87
ZnPorT8/Cu(II)	2 μM	20 μM	0.59